

# BD-simulated data for the paper:

”Ionic Coulomb blockade and anomalous mole fraction effect in the NaChBac bacterial ion channel and its charge-varied mutants”

I.Kh. Kaufman : Physics, Lancaster University, UK

O.A. Fedorenko : Biomedical and Life Sciences, Lancaster University, UK

D.G. Luchinsky : Physics, Lancaster University, UK and SGT, Inc.; Greenbelt, MD, 20770, US

W.A.T. Gibby : Physics, Lancaster University, UK

S.K. Roberts : Biomedical and Life Sciences, Lancaster University, UK

P.V.E. McClintock : Physics, Lancaster University, UK

R.S. Eisenberg : Molecular Biophysics, Rush University, Chicago, IL, US

August 1, 2017

## Abstract

We present a dataset for Brownian dynamic (BD) simulation of calcium Ca and sodium Na current  $J$  and occupancy  $P$  in dependence on the selectivity filter net fixed charge  $Q_f$  and bulk ionic concentrations  $[Ca]$  and  $[Na]$ .

## 1 Introduction

Biological ion channels are natural nanopores providing for the fast and highly selective permeation of physiologically important ions (e.g.  $Na^+$ ,  $K^+$  and  $Ca^{2+}$ ) through cellular membranes [1–3]. Despite its fundamental importance, and notwithstanding enormous efforts by numerous scientists, the physical origins of their selectivity still remain unclear. It is known, however, that the conduction and selectivity properties of cation channels are defined by the ions’ movements and interactions inside a short, narrow selectivity filter (SF) lined by negatively charged amino acid residues that provide a net fixed charge  $Q_f$  [1, 2].

Conduction and selectivity in calcium/sodium ion channels have recently been described [4–6] in terms of ionic Coulomb blockade (ICB) [7, 8], a fundamental electrostatic phenomenon based on charge discreteness, an electrostatic exclusion principle, and single-file stochastic ion motion through the channel. Earlier, Von Kitzing had revealed the staircase-like shape of the occupancy *vs* site affinity for the charged ion channel [9] (following discussions and suggestions in [10]), and comparable low-barrier ion-exchange transitions had been discovered analytically [11].

Here we present a results of Brownian dynamics (BD) simulations related to figures in [12]

In what follows  $\epsilon_0$  is the permittivity of free space,  $e$  is the proton charge,  $z$  is the ionic valence,  $T$  the temperature and  $k_B$  is Boltzmann’s constant.

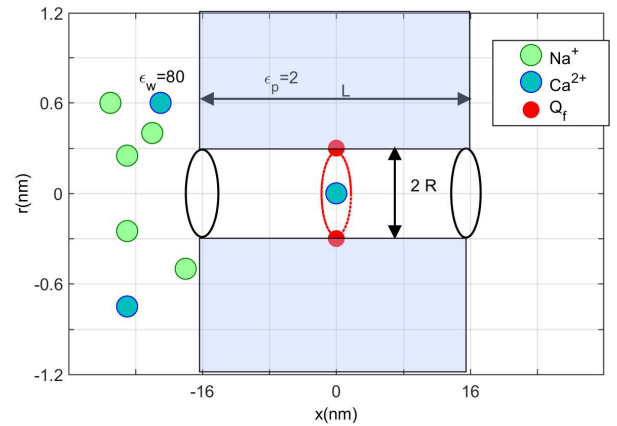


Figure 1: Generic electrostatic model of calcium/sodium ion channel [5]. The model describes the channel’s selectivity filter as an axisymmetric, water-filled pore of radius  $R = 0.3\text{nm}$  and length  $L = 1.6\text{ nm}$  through a protein hub embedded in the cellular membrane. A centrally-placed, uniform, rigid ring of negative charge  $Q_f$  is embedded in the wall to represent the charged residues of real  $Ca^{2+}/Na^+$  channels. We take both the water and the protein to be homogeneous continua describable by relative permittivities  $\epsilon_w = 80$  and  $\epsilon_p = 2$ , respectively, together with an implicit model of ion hydration whose validity is discussed elsewhere. The moving monovalent  $Na^+$  and divalent  $Ca^{2+}$  ions are assumed to obey self-consistently both Poisson’s electrostatic equation and the Langevin equation of motion.

## 2 Generic electrostatic model of Calcium/Sodium ion channel

Figure 1 summarises the generic, self-consistent, electrostatic model of the selectivity filter of a calcium/sodium channel introduced earlier [5]. It consists of a negatively-charged, axisymmetric, water-filled, cylindrical pore through the protein hub in the cellular membrane; and, we suppose it to be of radius  $R = 0.3\text{ nm}$  and length  $L = 1.6\text{ nm}$  [13], to match the dimensions of the selectivity filters of  $Na^+/Ca^{2+}$  channels.

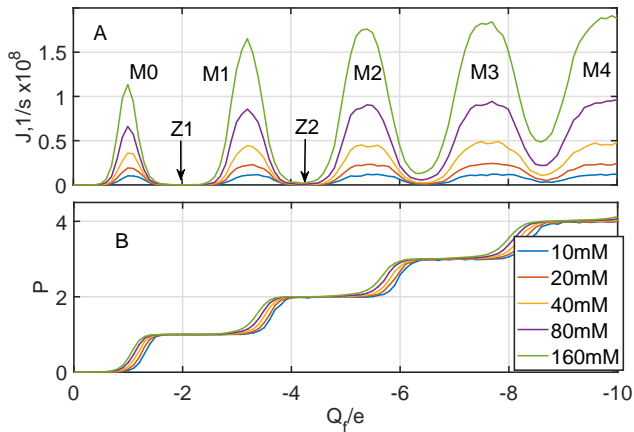


Figure 2: Multi-ion  $\text{Ca}^{2+}$  conduction/occupancy bands in the model calcium/sodium channel, showing occupancy shifts with ionic concentration. [A: "J\_Ca.dat"] Strong multi-ion calcium conduction bands  $M_n$  as established by Brownian dynamics simulations. The neutralized states  $Z_n$  providing blockade are interleaved with resonant states  $M_n$ . [B: "P\_Ca.dat"] The corresponding Coulomb staircase of occupancy  $P_c$  for different values of the extracellular calcium concentration  $[Ca]$ , as marked, consists of steps in occupancy that shift slightly as  $[Ca]$  changes.

There is a centrally-placed, uniformly-charged, rigid ring of negative charge  $0 \leq |Q_f/e| \leq 10$  embedded in the wall at  $R_Q = R$  to represent the charged protein residues of real  $\text{Ca}^{2+}/\text{Na}^+$  channels. The left-hand bath, modeling the extracellular space, contains non-zero concentrations of  $\text{Ca}^{2+}$  and/or  $\text{Na}^+$  ions.

For the Brownian dynamics simulations, we used a computational domain length of  $L_d = 10$  nm and radius  $R_d = 10$  nm, a grid size of  $h = 0.05$  nm. A potential difference in the range  $0 - 25$  mV (corresponding to the depolarized membrane state) was applied between the left and right domain boundaries. We take both the water and the protein to be homogeneous continua describable by relative permittivities  $\epsilon_w = 80$  and  $\epsilon_p = 2$ , respectively, together with an implicit model of ion hydration whose validity is discussed elsewhere [5]. These model parameters are assumed to be appropriate for the NaChBac channel, both for the wild type and for its mutants [14].

### 3 Self-consistent electrostatics-driven Brownian dynamics simulations

Electrostatic calculations have been performed with the use of Finite Volume Poisson Solver [15]. The BD simulations [5] were based on numerical solution of the 1D over-damped time-discretized Langevin equation for the  $i$ -th ion:

$$\frac{dx}{dt} = -Dz \left( \frac{\partial U}{\partial x} \right) + \sqrt{2D} \xi(t) \quad (1)$$

where  $D$  is the ionic diffusion coefficient,  $\xi(t)$  is normalized white noise,  $z$  is the valence of the ion, and the

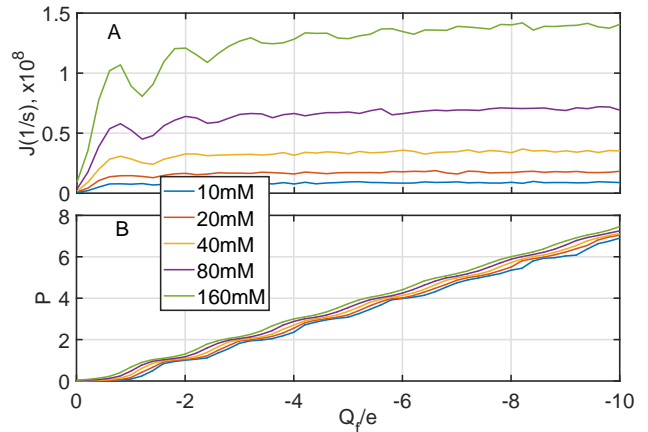


Figure 3: Multi-ion  $\text{Na}^+$  conduction/occupancy bands in the model calcium/sodium channel, showing occupancy shifts with ionic concentration. [A: "J\_Na.dat"] Weak multi-ion sodium conduction bands  $M_n$  as established by Brownian dynamics simulations. [B: "P\_Na.dat"] The corresponding occupancy  $P_c$  is an almost-washed-out Coulomb staircase whose steps shift slightly as the extracellular sodium concentration  $[Na]$  changes.

potential  $U(x)$  is given in  $(k_B T/e)$  units. Numerical solution of (1) was implemented with the Euler forward scheme. Poisson's equation is solved self-consistently at each simulation step.

We use an ion injection scheme that allows us to avoid wasteful and heavy-duty simulation of ionic movements in the bulk liquid. The model includes a hemisphere of radius  $R_a = R$  at each entrance representing the boundaries between the channel vicinity and the baths. The arrival rate  $j_{\text{arr}}$  is connected to the bulk concentration  $C$  through the Smoluchowski diffusion rate:  $j_{\text{arr}} = 2\pi D R_a C$  [16–18].

The motion of each injected ion is simulated in accordance with (1) until it reaches a domain boundary, where it is assumed to be absorbed. The simulation continues until a chosen simulation time has been reached. The ionic current  $J$  is calculated as the averaged difference between the numbers of similar ions passing the central cross-section of the channel per second in the forward and reverse directions [19].

Quantities measured during the simulations include the sodium  $J_{\text{Na}}$  and calcium  $J_{\text{Ca}}$  ion currents, the partial ionic occupancy profiles  $\rho(x)$  along  $x$  for different concentrations, and the partial  $P_{\text{Na}}$  and  $P_{\text{Ca}}$  occupancies, in each case as functions of the respective concentrations of calcium  $[Ca]$  or sodium  $[Na]$ .

The BD simulations of ion current  $J$  and occupancy  $P$  were performed separately for  $\text{CaCl}_2$  and  $\text{NaCl}$  solutions, with concentrations  $[Na, Ca]$  from 10mM to 160mM. The value of  $Q_f$  was varied within the range  $0-10e$  in order to cover the known mutants of sodium and calcium channels ([20]).

### 4 Model limitations

Of course, our reduced model represents a significant simplification of the actual electrostatics and dynam-

ics of ions and water molecules within the narrow selectivity filter due to, for example: the application of continuum electrostatics; the use of the implicit solvent model; and the assumption of 1D (i.e. single-file) movement of ions inside the selectivity filter. The validity and range of applicability of this kind of model have been discussed in detail elsewhere [5, 6, 21].

## 5 BD simulations results

Figure 2 presents the results of Brownian dynamics simulation of  $\text{Ca}^{2+}$  conduction and occupancy over an extended range of  $Q_f$  ( $0 - 10e$ ). Plot A shows strong oscillations of the conductance (conduction bands [4]); Plot B shows the corresponding occupancy  $P$ , which forms a Coulomb staircase, as predicted by the ICB model [6]. Plot B also reveals concentration-related shifts of the staircase.

Figure 3 presents a comparable set of Brownian dynamics results for the  $\text{Na}^+$  conduction and occupancy. Plot A shows weaker conductance oscillations (conduction bands [4]); Plot B shows the corresponding occupancy  $P$ , which forms a partly washed-out Coulomb staircase, as predicted by the ICB model [6]. Plot B also shows concentration-related shifts of the staircase.

## 6 Data files

Data is presented in simple space-separated ASCII files for Value-vs- $Q_f$ , where Value= $\{J,P\}$ , J is ionic current and P is the selectivity filter occupancy. First row defines  $Q_f$  grid in e-units, first column defines concentrations  $[X]$  grid in mM, where  $X=\{\text{Ca}, \text{Na}\}$ . Values for current are in ions/s.

"J\_Ca.dat" Ca current J vs  $Q_f$

"P\_Ca.dat" Ca occupancy P vs  $Q_f$

"J\_Na.dat" Na current J vs  $Q_f$

"P\_Na.dat" Na occupancy P vs  $Q_f$

## Conclusions

We presents two datasets with BD simulations for Ca and Na ions. BD simulations show multi-ion conduction bands, Coulomb staircase an concentration-related shifts.

## Acknowledgements

The research was supported by the UK Engineering and Physical Sciences Research Council [grant No. EP/M015831/1, "Ionic Coulomb blockade oscillations and the physical origins of permeation, selectivity, and their mutation transformations in biological ion channels"].

## References

- [1] B. Hille, *Ion Channels Of Excitable Membranes*, 3rd edn. (Sinauer Associates, Sunderland, MA, 2001)
- [2] J. Zheng, M.C. Trudeau (eds.), *Handbook of Ion Channels* (CRC Press Taylor & Francis Group, Boca Raton, FL, 2015)
- [3] B. Eisenberg, *Physiol.* **28**(1), 28 (2013)
- [4] I.K. Kaufman, D.G. Luchinsky, R. Tindjong, P.V.E. McClintock, R.S. Eisenberg, *Phys. Biol.* **10**(2), 026007 (2013)
- [5] I.K. Kaufman, D.G. Luchinsky, R. Tindjong, P.V.E. McClintock, R.S. Eisenberg, *Phys. Rev. E* **88**(5), 052712 (2013)
- [6] I.K. Kaufman, P.V.E. McClintock, R.S. Eisenberg, *New J. Phys.* **17**(8), 083021 (2015)
- [7] M. Krems, M. Di Ventra, *J. Phys. Condens. Matter* **25**, 065101 (2013)
- [8] J. Feng, K. Liu, M. Graf, D. Dumcenco, A. Kis, M. Di Ventra, A. Radenovic, *Nature Mater.* **15**(8), 850 (2016)
- [9] E. von Kitzing, in *Membrane Proteins: Structures, Interactions and Models: Proc. 25th Jerusalem Symposium on Quantum Chemistry and Biochemistry, Jerusalem, May 18-21, 1992*, ed. by A. Pullman, J. Jortner, B. Pullman (Kluwer, Dordrecht, 1992), pp. 297–314
- [10] R.S. Eisenberg, in *New Developments in Theoretical Studies of Proteins*, ed. by R. Elber (World Scientific, Singapore, 1996), pp. 269–357
- [11] J. Zhang, A. Kamenev, B.I. Shklovskii, *Phys. Rev. E* **73**, 051205 (2006)
- [12] I.K. Kaufman, O.A. Fedorenko, D.G. Luchinsky, W.A.T. Gibby, S.K. McClintock, R.S. Eisenberg, arXiv preprint arXiv:1612.02744 (2016)
- [13] B. Corry, T.W. Allen, S. Kuyucak, S.H. Chung, *Biophys. J.* **80**(1), 195 (2001)
- [14] C. Guardiani, P.M. Rodger, O.A. Fedorenko, S.K. Roberts, I.A. Khovanov, *J. Chem. Theor. Comp.* p. 10.1021/acs.jctc.6b01035 (2016). DOI 10.1021/acs.jctc.6b01035
- [15] I.K. Kaufman. Finite volume Poisson solver. Matlab Central (2009). URL [www.mathworks.co.uk/matlabcentral/fileexchange/25318-finite-volume-poisson-solver](http://www.mathworks.co.uk/matlabcentral/fileexchange/25318-finite-volume-poisson-solver)
- [16] B. Nadler, T. Naeh, Z. Schuss, *SIAM J. Appl. Math.* **62**(2), 433 (2001)
- [17] B. Nadler, U. Hollerbach, R.S. Eisenberg, *Phys. Rev. E* **68**(2, Part 1), 021905 (2003)

- [18] D.G. Luchinsky, R. Tindjong, I.K. Kaufman, P.V.E. McClintock, R.S. Eisenberg, in *Electrostatics 2007*, *J. Phys. Conf. Series*, vol. 142, ed. by Green, N. (2009), *J. Phys. Conf. Series*, vol. 142
- [19] S.O. Yesylevskyy, V.N. Kharkyanen, *Chem. Phys.* **312**, 127 (2005)
- [20] E. Csányi, D. Boda, D. Gillespie, T. Kristf, *Biochim. Biophys. Acta (BBA) – Biomembranes* **1818**(3), 592 (2012)
- [21] B. Roux, T. Allen, S. Berneche, W. Im, *Quart. Rev. Biophys.* **37**(1), 15 (2004)